# Application of Surface-Stress Driven Model for Higher Vibrations Modes of Functionally Graded Nanobeams

Giuseppe Lovisi * , Luciano Feo , Annavirginia Lambiase , And Rosa Penna

Posted Date: 10 January 2024

doi: 10.20944/preprints202401.0738.v1

Keywords: Functionally Graded (FG) Materials; Bernoulli-Euler Nanobeams; Stress-Driven Nonlocal Model; Free Vibration Analysis; Surface Energy Effects; Higher Vibration Modes

*Article*

# Application of Surface-Stress Driven Model for Higher Vibrations Modes of Functionally Graded Nanobeams

**Giuseppe Lovisi*, Luciano Feo, Annavirginia Lambiase, and Rosa Penna**

Department of Civil Engineering, University of Salerno, 84084 Fisciano, Italy; glovisi@unisa.it (G.L.); lfeo@unisa.it (L.F.); annlambiase@unisa.it (A.L.); rpenna@unisa.it (R.P.).

* Correspondence: glovisi@unisa.it; Tel.: +39-089964209

**Abstract:** This paper employs a surface stress-driven nonlocal theory to investigate the synergistic impact of long-range interaction and surface energy on higher vibration modes of Bernoulli-Euler nanobeams made of functionally graded material taking into account surface effects, such as surface modulus of elasticity, residual surface stresses, surface density, and rotary inertia. The governing equation is derived through the application of Hamilton's principle. The study conducts a parametric investigation, examining the effects of nonlocal parameter and the material gradient index for four static schemes. The outcomes are presented and discussed, highlighting the normalized nonlocal natural frequencies for the second through fifth mode of vibrations in each case under study.

**Keywords:** functionally graded materials; bernoulli-euler nanobeams; surface stress-driven nonlocal model; free vibration analysis; surface energy effects; higher vibration modes

## 1. Introduction

The last decades have seen significant progress in the field of nanoscience and nanotechnology, leading the scientific community to focus extensively on the analysis, modelling and development of nanostructures [1–3]. Nanostructures are now employed in various fields and it is crucial to have accurate models for their reliable and efficient design. Further progress has been made with the introduction of functionally graded materials (FG) in the field of nanostructures, allowing them to maintain high performance even under conditions of high thermal and mechanical stress [4–6].

Hence, understanding the size-dependent behavior of these nanostructures is essential, considering their broad application in nanomechanical devices such as nanoelectromechanical actuators and nanomechanical resonators [7,8].

As commonly recognized, when the size of a structure reduces to the nanoscale, small-scale phenomena, negligible at the macro-scale, become predominant. In particular, atomic interaction and surface effects play a crucial role that cannot be neglected at the nanoscale.

Various approaches exist for the study of nanostructures, including experimental investigations and molecular dynamics simulations [9,10]. Both are characterized by high computational costs and long analysis times.

In recent years, researchers have explored the introduction of non-classical continuum models for the study of nanostructures, appropriately modified to capture long-range interactions and surface effects.

One of the earliest non-classical continuum models is the Eringen [11] one, which differs from the classical continuum formulation by assuming that the stress at a point also depends on the deformation of the surrounding points. Eringen proposed a theory to capture this effect, where the stress field is obtained through an integral convolution, driven by strain, between the elastic strain field and an averaging kernel. To overcome the mathematical difficulties of integral resolution,

 doi:10.20944/preprints202401.0738.v1



Eringen later proposed the equivalent differential formulation (EDM) [12]. Additional nonlocal models have been developed from this formulation, including the nonlocal Eringen mixture model [13] and the nonlocal Lim gradient strain model [14], obtained by coupling the EDM model with the Mindlin gradient model [15].

In addition, Gurtin and Murdoch [16,17] introduced Surface Elasticity Theory (SET) to address the effects of surface energy. In this theory the surface layer is considered as a membrane of negligible thickness, perfectly adhering to the mass continuum, and characterized by unique properties and constitutive laws distinct from those that govern the volume. This theory has often been coupled with the Eringen model to capture not only nonlocal effects but also surface effects.

Although these models have been widely used to study the static and dynamic aspect of nanostructures, the scientific community considers these models inapplicable for the study of structures whose results are known as nanomechanics paradoxes [18–21].

To overcome the mathematical inconsistencies of the aforementioned models, Ro-mano and Barretta proposed a new Stress-Driven Model (SDM) of nonlocal elasticity [22], in which the integral convolution is a function of the stress field instead of the strain one. It has been extensively used in recent years to study both the static and the dynamic response of functionally graded nanobeams subjected to thermos-mechanical stresses [23–34].

Furthermore, Penna [35] recently extended the SDM model by coupling it with the SET theory to create the Surface Stress-Driven Model (SSDM). This model, well-posed mathematically, not only captures long-range interactions but also addresses surface effects. This new model has been recently used to investigate the free vibrations of functionally graded nanobeams [36], analyze static response in the presence of discontinuous loads [37], and investigate the effects of cracks in FG nanobeams [38].

The main innovation of this manuscript lies in the pioneering use of the SSDM model to determine the frequencies of higher vibration modes. Specifically, it explores the effects of the nonlocal parameter, surface energy, and material gradient index on the natural frequency of the FG nanobeam, focusing on higher vibration modes for both rectangular and circular cross-sectional shapes.

The document's structure is the following: in Section 2, the problem formulation is provided, including kinematics, geometry, material, and the governing equations of free oscillations derived from the use of the Hamilton's Principle. A brief description of the SSDM model and the dimension-dependent governing equations of transverse free oscillations are presented in Section 3. In the parametric analysis outlined in Section 4, we investigate and discuss the combined influences of the nonlocal parameter, surface effects, and gradient index on the higher-order vibration modes of the four considered static schemes. Finally, in Section 5, some concluding remarks are provided.

**Nomenclature**

| | | | |
|---|---|---|---|
| | | $\lambda_c$ | Nonlocal parameter |
| | | $\nu^B, \nu^S$ | Poisson's ratios of the bulk and surface layer |
| E | Euclidean space | $n$ | material gradient index |
| $L$ | Length of FG nanobeam | $E_c$ | Young's modulus ceramic |
| $\Sigma$ | Generic cross-section | $E_m$ | Young's modulus metal |
| $\partial\Sigma$ | Perimeter of $\Sigma$ | $\rho_c$ | Mass density of ceramic |
| $\{O, x, y, z\}$ | Cartesian coordinate system | $\rho_m$ | Mass density of metal |
| $O$ | Geometric center of $\Sigma$ | $E_c^S$ | Surface Young modulus of ceramic |
| $x$ | Axis of FG nanobeam | $E_m^S$ | Surface Young modulus of metal |
| $y$, $z$ | Principal axes of geometric inertia of $\Sigma$ | $\rho_c^S$ | Surface mass density of ceramic |
| $b$, $h$ | Width and thickness $\Sigma$ | $\rho_m^S$ | Surface mass density of metal |
| $R$ | Radius of $\Sigma$ | $\tau_c^S$ | Residual surface stress of ceramic |
| $B$, $S$ | Bulk and surface layers of FG material | $\tau_m^S$ | Residual surface stress of metal |

Preprints (www.preprints.org) | NOT PEER-REVIEWED | Posted: 10 January 2024 doi:10.20944/preprints202401.0738.v1



## 2. Problem formulation

Figure 1 shows the coordinate system and configuration of the FG nanobeam under investigation, composed of a bulk volume (B), made of a mixture of metal ($m$) and ceramic ($c$), and a thin surface layer ($S$), perfectly adhered to the bulk continuum (refer to Figure 1) with two distinct cross-sectional shapes.

As it is well-known, for a Bernoulli-Euler FG nanobeam whose mechanical and physical properties vary along the thickness ($z$), it can be assumed that the bulk elastic modulus of elasticity, $E^B = E^B(z)$, the surface modulus of elasticity, $E^S = E^S(z)$, the residual surface stress, $\tau^S = \tau^S(z)$, the bulk mass density, $\rho^B = \rho^B(z)$, and the surface mass density, $\rho^S = \rho^S(z)$, follow a power-law functions as given below [39]

$$E^B(z) = E_m + (E_c - E_m)\left(\frac{1}{2} + \frac{z}{\zeta}\right)^n \tag{1}$$

$$E^S(z) = E_m^S + (E_c^S - E_m^S)\left(\frac{1}{2} + \frac{z}{\zeta}\right)^n \tag{2}$$

$$\tau^S(z) = \tau_m^S + (\tau_c^S - \tau_m^S)\left(\frac{1}{2} + \frac{z}{\zeta}\right)^n \tag{3}$$

$$\rho^B(z) = \rho_m + (\rho_c - \rho_m)\left(\frac{1}{2} + \frac{z}{\zeta}\right)^n \tag{4}$$

$$\rho^S(z) = \rho_m^S + (\rho_c^S - \rho_m^S)\left(\frac{1}{2} + \frac{z}{\zeta}\right)^n \tag{5}$$

being $n$ the material gradient index ($n \geq 0$); $\zeta$=$h$, in the case of a rectangular cross-section and $\zeta$=$2R$, for a circular one. Poisson's ratio is here assumed to be constant ($\nu^B = \nu^S = \nu$).

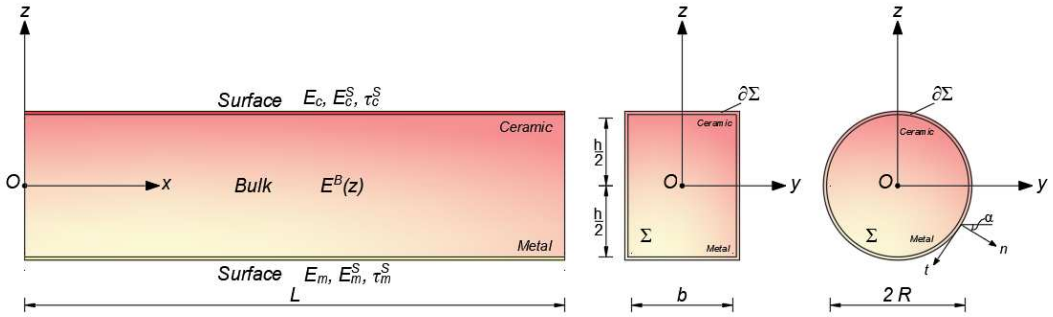


**Figure 1.** Coordinate system and configuration of the FG nanobeam: bulk continuum and surface layer.

### 2.1. Kinematic

The Bernoulli-Euler beam theory considers the following displacement field

$$\boldsymbol{u}(\boldsymbol{x}, t) = u_x(x, z, t)\hat{\boldsymbol{e}}_{\boldsymbol{x}} + u_z(x, z, t)\hat{\boldsymbol{e}}_{\boldsymbol{z}} \tag{6}$$

where $\hat{\boldsymbol{e}}_{\boldsymbol{x}}$ and $\hat{\boldsymbol{e}}_{\boldsymbol{z}}$ are, respectively, the unit vectors along $x$- and $z$-axes; $u_x(x, z, t)$ and $u_z(x, z, t)$ indicate the Cartesian components of the displacement field along $x$ and $z$ axes at time $t$, expressed as follows

$$u_x(x, z, t) = -z\frac{\partial w(x, t)}{\partial x} \tag{7}$$

$$u_z(x, z, t) = w(x, t) \tag{8}$$

being $w(x, t) = w$ the transverse displacement of the geometric center $O$ (at time $t$). Within the assumptions of the small strain and displacement theory, the simplified Green-Lagrange strain tensor is

$$\boldsymbol{E} \approx \boldsymbol{\varepsilon} = \varepsilon_{xx}\,\hat{\boldsymbol{e}}_{\boldsymbol{x}}\hat{\boldsymbol{e}}_{\boldsymbol{x}} \tag{9}$$

where

Preprints (www.preprints.org) | NOT PEER-REVIEWED | Posted: 10 January 2024 doi:10.20944/preprints202401.0738.v1



$$\varepsilon_{xx} = \varepsilon_{xx}(x,z,t) = -z\frac{\partial^2 w(x,t)}{\partial x^2} \tag{10}$$

being $\frac{\partial^2 w(x,t)}{\partial x^2}$ the geometric bending curvature $\chi$.

*2.2. Governing equations*

The use of Hamilton's principle allows us to obtain the governing equation of the free vibrations problem [36]

$$\frac{\partial^2 M}{\partial x^2} + T^S\frac{\partial^2 w}{\partial x^2} = \left(A_\rho^B + A_\rho^S\right)\frac{\partial^2 w}{\partial t^2} - \left(I_\rho^B + I_\rho^S\right)\frac{\partial^4 w}{\partial x^2 \partial t^2} \tag{11}$$

where

$$\left\{A_\rho^B, I_\rho^B\right\} = \int_\Sigma \rho^B \{1, z^2\} d\Sigma \tag{12}$$

$$\left\{A_\rho^S, I_\rho^S\right\} = \oint_{\partial\Sigma} \rho^S \{1, z^2\} d\sigma \tag{13}$$

$$T^S = \begin{cases} \oint_{\partial\Sigma} \tau^S d\sigma & (rectangular\ cross-section) \\ \oint_{\partial\Sigma} \tau^S n_z d\sigma & (circular\ cross-section) \end{cases} \tag{14}$$

being $n_z$ the z-component of the unit normal vector $\boldsymbol{n}$, which is the outward normal to the cross-section lateral surface [35].

The appropriate boundary conditions of the FG nanobeam (at the nanobeam ends $x = 0,L$) can be determined by selecting a single condition from each of the two pairs of Standard Boundary Conditions (SBCs) [36]

$$[w]_{0,L} \quad \text{or} \quad \left[\frac{\partial M}{\partial x} + T^S\frac{\partial w}{\partial x} + \left(I_\rho^B + I_\rho^S\right)\frac{\partial^3 w}{\partial x \partial t^2}\right]_{0,L} \tag{15}$$

$$\left[\frac{\partial w}{\partial x}\right]_{0,L} \quad \text{or} \quad [M]_{0,L} \tag{16}$$

being $M$ the bending moment of FG nanobeam.

## 3. Surface stress-driven model for free vibrations analysis

*3.1. A brief outline of the surface stress-driven nonlocal model*

In this section, we provide a brief review of the surface stress-driven nonlocal model (SSDM) as outlined in [35]. Assuming a purely elastic constitutive behavior, the formulation of the surface stress-driven nonlocal model involves defining the bending curvature, $\chi$, through the integral convolution, as detailed in the same reference [35]

$$\chi = \int_0^L \Phi_{L_c}(x-\xi, L_c)\left(-\frac{M^*}{I_E^*}\right)d\xi \tag{17}$$

where $x$ and $\xi$ are the positions of points of the domain of the Euclidean space occupied by the FG nanobeam at time $t$; $\Phi_{L_c}$ is an averaging kernel depending on the characteristic length of material, $L_c = \lambda_c L$; $I_E^*$ and $M^*$ are, respectively, the equivalent bending stiffness and the applied bending moment, defined as

$$I_E^* = \int_\Sigma [E^B + \nu\, C]\, z^2 d\Sigma + \oint_{\partial\Sigma} E^S z^2\, d\sigma \tag{18}$$

$$M^* = M^*(x,t) = M - M^\tau - \Lambda\frac{\partial^2 w}{\partial t^2} \tag{19}$$

being

$$C = \frac{2}{h}\left[\left(\frac{z}{h}\right)^2 - \frac{3}{4}\right](\tau_c^S + \tau_m^S) - \frac{1}{2z}(\tau_c^S - \tau_m^S) \tag{20}$$

$$M^\tau = \oint_{\partial\Sigma} \tau^S z\, d\sigma \tag{21}$$

$$\Lambda = \int_\Sigma \nu\, D\, z\, d\Sigma \tag{22}$$

and

Preprints (www.preprints.org) | NOT PEER-REVIEWED | Posted: 10 January 2024 doi:10.20944/preprints202401.0738.v1



$$D = 2\frac{z}{h}\left[\left(\frac{z}{h}\right)^2 - \frac{3}{4}\right](\rho_c^S + \rho_m^S) - \frac{1}{2}(\rho_c^S + \rho_m^S) \tag{23}$$

As widely recognized, a specific function kernel, denoted as $\Phi_{L_c}$, is chosen to be

$$\Phi_{L_c}(x, L_c) = \frac{1}{2L_c}\exp\left(-\frac{|x|}{L_c}\right) \tag{24}$$

for smooth source fields $\left(-\frac{M^*}{I_E^*}\right)$ in the domain $[0, L]$, the elastic curvature $\chi$, as expressed in Eq.17, is equivalent to the following second-order differential equations, as outlined in [35]

$$\left(1 - L_c^2\frac{\partial^2}{\partial x^2}\right)\chi = -\frac{M^*}{I_E^*} \tag{25}$$

This equivalence is true if and only if the conventional Constitutive Boundary Conditions (CBCs) of the stress-driven nonlocal theory are satisfied at the ends of the FG nanobeam

$$\frac{\partial\chi(0)}{\partial x} - \frac{1}{L_c}\chi(0) = 0 \tag{26}$$

$$\frac{\partial\chi(L)}{\partial x} + \frac{1}{L_c}\chi(L) = 0 \tag{27}$$

By manipulating Eq. 25, we can derive the expression for the resultant bending moment in the surface stress-driven nonlocal model

$$M = M(x,t) = -(I_E^B + I_E^S)\frac{\partial^2 w}{\partial x^2} + (I_E^B + I_E^S)L_c^2\frac{\partial^4 w}{\partial x^4} + M^\tau + \Lambda\frac{\partial^2 w}{\partial t^2} \tag{28}$$

*3.2. Size-dependent governing equation*

By inserting Eq.28 into Eq.11, we obtain the equation that governs the dynamic problem of the FG nanobeam, incorporating both nonlocal and surface energy effects

$$(I_E^B + I_E^S)L_c^2\frac{\partial^6 w}{\partial x^6} - (I_E^B + I_E^S)\frac{\partial^4 w}{\partial x^4} + T^S\frac{\partial^2 w}{\partial x^2} = \left(A_\rho^B + A_\rho^S\right)\frac{\partial^2 w}{\partial t^2} - \Lambda\frac{\partial^4 w}{\partial x^2\partial t^2} - \left(I_\rho^B + I_\rho^S\right)\frac{\partial^4 w}{\partial x^2\partial t^2} \tag{29}$$

with the corresponding standard (Eqs. 15 and 16) and constitutive (Eqs. 26 and 27) boundary conditions at the FG nanobeam ends ($x = 0, L$).

Conclusively, by introducing the following dimensionless quantities

$$\tilde{x} = \frac{x}{L} \qquad \tilde{w} = \frac{w}{L} \qquad \lambda_c = \frac{L_c}{L} \qquad \tilde{M}^\tau = \frac{M^\tau L}{I_E^*}$$

$$\tilde{T}^S = \frac{T^S L^2}{I_E^*} \qquad \tilde{A}_\rho^B = \frac{A_\rho^B L^4}{I_E^*} \qquad \tilde{A}_\rho^S = \frac{A_\rho^S L^4}{I_E^*} \qquad \tilde{I}_\rho^B = \frac{I_\rho^B L^2}{I_E^*} \qquad \tilde{I}_\rho^S = \frac{I_\rho^S L^2}{I_E^*} \tag{30}$$

$$\tilde{\Lambda} = \frac{1}{L^2}\frac{\Lambda}{A_\rho^B} \qquad \tilde{g}^B = \frac{1}{L^2}\frac{I_\rho^B}{A_\rho^B} \qquad \tilde{g}^S = \frac{1}{L^2}\frac{I_\rho^S}{A_\rho^B} \qquad \tilde{r} = \frac{A_\rho^S}{A_\rho^B} \qquad \tilde{\Lambda} = \frac{1}{L^2}\frac{\Lambda}{A_\rho^B}$$

and by using the classical method of separation variables, in which ω indicates the natural nonlocal frequency of transverse vibrations

$$\tilde{w}(\tilde{x}, t) = \widetilde{W}(\tilde{x})e^{i\omega t} \tag{31}$$

the dimensionless equation governing the linear transverse free vibrations based on SSDM can be expressed in terms of the non-dimensional spatial shape $\widetilde{W} = \widetilde{W}(\tilde{x})$, as follows

$$\lambda_c^2\frac{\partial^6\widetilde{W}}{\partial\tilde{x}^6} - \frac{\partial^4\widetilde{W}}{\partial\tilde{x}^4} + \tilde{T}^S\frac{\partial^2\widetilde{W}}{\partial\tilde{x}^2} = \tilde{\omega}^2\left(\left(\tilde{\Lambda} + \tilde{g}^B + \tilde{g}^S\right)\frac{\partial^2\widetilde{W}}{\partial\tilde{x}^2} - (1 + \tilde{r})\widetilde{W}\right) \tag{32}$$

being

$$\tilde{\omega}^2 = \tilde{A}_\rho^B\omega^2 \tag{33}$$

with the corresponding dimensionless standard and constitutive boundary conditions

$$\left[\widetilde{W}\right]_{\tilde{x}=0,1} \quad \text{or} \quad \left[\frac{\partial\widetilde{M}}{\partial\tilde{x}} + \tilde{T}^S\frac{\partial\widetilde{W}}{\partial\tilde{x}} + (\tilde{g}^B + \tilde{g}^s)\frac{\partial\widetilde{W}}{\partial\tilde{x}}\right]_{\tilde{x}=0,1} \tag{34}$$

$$\left[\frac{\partial\widetilde{W}}{\partial\tilde{x}}\right]_{\tilde{x}=0,1} \quad \text{or} \quad \left[\widetilde{M}\right]_{\tilde{x}=0,1} \tag{35}$$

$$-\frac{\partial^3\widetilde{W}(0)}{\partial\tilde{x}^3} + \frac{1}{\lambda_c}\frac{\partial^2\widetilde{W}(0)}{\partial\tilde{x}^2} = 0 \tag{36}$$

$$-\frac{\partial^3\widetilde{W}(1)}{\partial\tilde{x}^3} - \frac{1}{\lambda_c}\frac{\partial^2\widetilde{W}(1)}{\partial\tilde{x}^2} = 0 \tag{37}$$

Preprints (www.preprints.org) | NOT PEER-REVIEWED | Posted: 10 January 2024 doi:10.20944/preprints202401.0738.v1



being $\widetilde{M}$ the dimensionless surface stress-driven nonlocal resultant moment expressed as follows

$$\widetilde{M} = \widetilde{M}(\tilde{x}) = \lambda_c^2 \frac{\partial^4 \widetilde{W}}{\partial \tilde{x}^4} - \frac{\partial^2 \widetilde{W}}{\partial \tilde{x}^2} + \widetilde{M}^{\tau} - \tilde{\omega}^2 \tilde{\Lambda}\, \widetilde{W} \tag{38}$$

Eq.32 admits the following solution

$$\widetilde{W} = \sum_{k=1}^{6} q_k e^{\tilde{x}\,\beta_k} \tag{39}$$

It is essential to underline that the determination of the six unknown constants, indicated as $q_k$, depends on the satisfaction of the boundary conditions specified in Eqs. 34-37. The linear fundamental natural frequencies of the FG nanobeam are established by addressing the eigenvalue problem articulated in a six-dimensional array $\boldsymbol{q} = \{q_1, .., q_6\}$.

## 4. Results and discussion

In this paragraph, a higher order free vibration analysis of Bernoulli-Euler FG nanobeam with length $L$ = 10 nm is developed by considering Cantilever (C-F), Simply-Supported (S-S), Clamped-Pinned (C-P) and Doubly-Clamped (C-C) static configurations.

The analysis has been conducted using both surface stress-driven model (SSDM) and stress-driven model (SDM) without considering the surface energy effects. In addition, the present study encompasses two distinct cross-sectional shapes having the same second moment of area about their principal axis of geometric inertia $y$: a square cross-section ($b$=$h$ = 0.1$L$ = 1nm) and a circular one of radius $R$=0.571nm.

The characteristic value of physical and elastic properties of the two constituent materials, in terms of bulk Young's modulus, $E_c^B$ and $E_m^B$, surface Young's modulus, $E_c^S$ and $E_m^S$, residual surface stress, $\tau_c^S$ and $\tau_m^S$, bulk mass density, $\rho_c^B$ and $\rho_m^B$, and surface mass density, $\rho_c^S$ and $\rho_m^S$, are summarized in the following Table 1 [35].

**Table 1.** Physical and elastic properties of the two constituent materials of FG nanobeam.

| Material | Parameters | Values | Unit |
|---|---|---|---|
| Ceramic (Si) | $E_c^B$ | 210 | [GPa] |
| | $E_c^S$ | -10.6543 | [N/m] |
| | $\tau_c^S$ | 0.6048 | [N/m] |
| | $\rho_c^B$ | 2370 | [kg/m$^3$] |
| | $\rho_c^S$ | 3.1688 $10^{-7}$ | [kg/m$^2$] |
| Metal (Al) | $E_m^B$ | 70 | [GPa] |
| | $E_m^S$ | 5.1882 | [N/m] |
| | $\rho_m^B$ | 2700 | [kg/m$^3$] |
| | $\tau_m^S$ | 0.9108 | [N/m] |
| | $\rho_m^S$ | 5.4610 $10^{-7}$ | [kg/m$^2$] |

The following results are expressed in terms of dimensionless normalized nonlocal frequency, obtained as the ratio between the nonlocal dimensionless frequency (Eq. 31) and the dimensionless local frequency $\tilde{\omega}_{loc}^2$. The dimensionless local frequency, $\tilde{\omega}_{loc}^2$, is the natural frequency of the first order (obtained by setting $\lambda_c = \tilde{g}^B = \tilde{g}^S = \tilde{\Lambda} = \tilde{r} = \tilde{T}^S = n = 0$) and is assumed to be equal to 3.5160 for Cantilever FG nanobeam, 9.8696 for Simply-Supported, 15.4182 for Clamped-Pinned and 22.3733 for Doubly-Clamped.

Firstly, in Tables 2-5 the present approach has been validated by comparing the corresponding results, in terms of dimensionless nonlocal frequencies, to those obtained by Raimondo et al. in Ref. [34] for homogenous nanobeams by neglecting both the surface energy effects and the gyration radius ($\tilde{g}^B = 0$).

Tables 2-5 provide a summary of the results of the free vibration analysis in terms of normalized nonlocal high frequencies, corresponding to $\lambda_c \in \{0.00^+, 0.01, 0.02, 0.03, 0.04, 0.05, 0.06, 0.07, 0.08, 0.09, 0.10\}$ and to $n \in \{0,1,3\}$ for the first five vibrations modes.

Looking at the results, it is evident that an increase in the material gradient index consistently leads to higher normalized nonlocal frequencies for the square cross-section, regardless of the

Preprints (www.preprints.org) | NOT PEER-REVIEWED | Posted: 10 January 2024 doi:10.20944/preprints202401.0738.v1



boundary constraints considered. However, for the circular cross-section the trend is conditioned by the specific static scheme considered.

Furthermore, from Tables 2-5 and Figures 2-5, it is easy to observe that the dimensionless nonlocal frequencies increase with increasing the order of the vibration modes for all the static schemes here considered. In addition, by fixing the values of nonlocal parameter and the material gradient index, it is observed that the dimensionless nonlocal frequencies reach their maximum value in the case of the Cantilever FG nanobeam and the minimum one in the case of Doubly-Clamped FG nanobeam for each vibration mode, regardless of the cross-sectional shapes chosen.

Therefore, it may be concluded that nonlocality strongly influences the normalized nonlocal frequencies, and its effects are stronger for higher vibrations modes. In fact, increasing the nonlocal parameter always shows an increase in the dimensionless nonlocal frequencies.

Moreover, in the case of a square cross-section, the presence of surface effects results in additional stiffness, leading to an increase in the normalized nonlocal frequencies for the first three vibration modes compared to the model without surface effects in Ref. [34]; however, the surface energy causes a reduction in normalized nonlocal frequencies for the fourth and fifth vibration modes. On the contrary, FG nanobeams characterized by a circular cross-section show a more general dynamic response. In fact, it depends on the intertwined effects of the nonlocal parameter and the material gradient index, together with the boundary conditions at the nanobeam ends.

Finally, in Figures 2-5, a comparison between the normalized nonlocal frequency curves for the surface stress-driven model (SSDM) and the stress-driven model (SDM) without surface effects is presented. The comparison spans all static configurations and the two types of cross sections considered. For these illustrations the parameters $\lambda\,\lambda_c = 0.05$ and $n = 1$ are set. As it can be observed, the SSDM consistently provides a stiffening behavior as the number of vibration modes increases.

**Table 2.** Dimensionless nonlocal frequencies of Cantilever (C-F) FG nanobeam for higher modes of vibrations.

| $\lambda_c$ | Mode | No Surface Effects | | Square Cross-Section | | | Circular Cross-Section | | |
|---|---|---|---|---|---|---|---|---|---|
| | | Present | Ref. [34] | $n=0$ | $n=1$ | $n=3$ | $n=0$ | $n=1$ | $n=3$ |
| $0.00^{+}$ | $1^{st}$ | 1.0000 | 1.0000 | 2.2799 | 2.7626 | 3.0027 | 1.4981 | 1.7904 | 1.8865 |
| | $2^{nd}$ | 6.2669 | 6.2669 | 8.5112 | 9.7142 | 10.3436 | 5.9107 | 6.7299 | 6.9369 |
| | $3^{th}$ | 17.5475 | 17.5475 | 19.1051 | 20.4685 | 21.2408 | 13.9919 | 15.2841 | 15.4319 |
| | $4^{th}$ | 34.3860 | - | 33.8579 | 35.1898 | 35.9955 | 25.6689 | 27.4754 | 27.5037 |
| | $5^{th}$ | 56.8427 | - | 51.8652 | 53.0981 | 53.9124 | 40.5012 | 42.7677 | 42.6559 |
| 0.01 | $1^{st}$ | 1.0101 | - | 2.2946 | 2.7797 | 3.0209 | 1.5081 | 1.8020 | 1.8985 |
| | $2^{nd}$ | 6.3357 | - | 8.5816 | 9.7884 | 10.4201 | 5.9625 | 6.7859 | 6.9931 |
| | $3^{th}$ | 17.7713 | - | 19.3130 | 20.6764 | 21.4494 | 14.1515 | 15.4522 | 15.5981 |
| | $4^{th}$ | 34.9207 | - | 34.3280 | 35.6554 | 36.4594 | 26.0392 | 27.8616 | 27.8852 |
| | $5^{th}$ | 57.9402 | - | 52.7813 | 54.0042 | 54.8148 | 41.2392 | 43.5319 | 43.4113 |
| 0.03 | $1^{st}$ | 1.0309 | - | 2.3244 | 2.8137 | 3.0569 | 1.5284 | 1.8254 | 1.9228 |
| | $2^{nd}$ | 6.5093 | - | 8.7539 | 9.9674 | 10.6034 | 6.0897 | 6.9227 | 7.1298 |
| | $3^{th}$ | 18.5002 | - | 19.9871 | 21.3409 | 22.1109 | 14.6669 | 15.9929 | 16.1306 |
| | $4^{th}$ | 37.0797 | - | 36.2703 | 37.5626 | 38.3510 | 27.5482 | 29.4378 | 29.4370 |
| | $5^{th}$ | 63.0858 | - | 57.2474 | 58.4058 | 59.1879 | 44.7714 | 47.2065 | 45.1013 |
| 0.05 | $1^{st}$ | 1.0524 | 1.0524 | 2.3545 | 2.8477 | 3.0926 | 1.5490 | 1.8491 | 1.9471 |
| | $2^{nd}$ | 6.7278 | 6.7278 | 8.9646 | 10.1836 | 10.8232 | 6.2460 | 7.0897 | 7.2959 |
| | $3^{th}$ | 19.5634 | 19.5634 | 20.9672 | 22.2996 | 23.0608 | 15.4154 | 16.7767 | 16.9002 |
| | $4^{th}$ | 40.4580 | - | 39.3323 | 40.5640 | 41.3229 | 29.9179 | 31.9145 | 31.8738 |
| | $5^{th}$ | 71.3062 | - | 64.4541 | 65.5116 | 66.2479 | 50.4474 | 53.1200 | 52.8692 |
| 0.10 | $1^{st}$ | 1.1087 | 1.1087 | 2.4306 | 2.9331 | 3.1817 | 1.6011 | 1.9090 | 2.0088 |
| | $2^{nd}$ | 7.4325 | 7.4325 | 9.6210 | 10.8467 | 11.4935 | 6.7369 | 7.6095 | 7.8101 |
| | $3^{th}$ | 23.2560 | 23.2560 | 24.3703 | 25.6113 | 26.3313 | 18.0146 | 19.4950 | 19.5662 |

Preprints (www.preprints.org) | NOT PEER-REVIEWED | Posted: 10 January 2024 doi:10.20944/preprints202401.0738.v1



| | | | | | | | | | |
|---|---|---|---|---|---|---|---|---|---|
| | $4^{th}$ | 52.1914 | - | 50.0444 | 51.0811 | 51.7429 | 38.1909 | 40.5729 | 40.3977 |
| | $5^{th}$ | 99.0703 | - | 88.9574 | 89.7452 | 90.3647 | 69.7106 | 73.2203 | 72.7155 |

**Table 3.** Dimensionless nonlocal frequencies of Simply-Supported (S-S) FG nanobeam for higher modes of vibrations.

| $\lambda_c$ / $\lambda_c$ | Mode | No Surface Effects | | Square Cross-Section | | | Circular Cross-Section | | |
|---|---|---|---|---|---|---|---|---|---|
| | | Present | Ref. [34] | $n=0$ | $n=1$ | $n=3$ | $n=0$ | $n=1$ | $n=3$ |
| | $1^{st}$ | 1.0000 | 1.0000 | 1.5375 | 1.8218 | 1.9718 | 1.0416 | 1.2124 | 1.2649 |
| | $2^{nd}$ | 4.0000 | 4.0000 | 4.4988 | 4.8850 | 5.1033 | 3.2633 | 3.5906 | 3.6395 |
| $0.00^{+}$ | $3^{th}$ | 9.0000 | 9.0000 | 9.0110 | 9.4167 | 9.6589 | 6.7903 | 7.2932 | 7.3111 |
| | $4^{th}$ | 16.0000 | - | 14.7940 | 15.1850 | 15.4386 | 11.4929 | 12.1644 | 12.1399 |
| | $5^{th}$ | 24.9999 | - | 21.5186 | 21.8782 | 22.1411 | 17.1945 | 17.9903 | 17.9198 |
| | $1^{st}$ | 1.0005 | - | 1.5379 | 1.8221 | 1.9721 | 1.0419 | 1.2127 | 1.2651 |
| | $2^{nd}$ | 4.0077 | - | 4.5052 | 4.8909 | 5.1090 | 3.2684 | 3.5953 | 3.6445 |
| 0.01 | $3^{th}$ | 9.0391 | - | 9.0449 | 9.4485 | 9.6905 | 6.8170 | 7.3206 | 7.3380 |
| | $4^{th}$ | 16.1233 | - | 14.8988 | 15.2869 | 15.5391 | 11.5764 | 12.2508 | 12.2248 |
| | $5^{th}$ | 25.3003 | - | 21.7635 | 22.1185 | 22.3792 | 17.3934 | 18.2228 | 18.1220 |
| | $1^{st}$ | 1.0042 | - | 1.5402 | 1.8240 | 1.9739 | 1.0438 | 1.2146 | 1.2669 |
| | $2^{nd}$ | 4.0662 | - | 4.5541 | 4.9359 | 5.1521 | 3.3068 | 3.6349 | 3.6824 |
| 0.03 | $3^{th}$ | 9.3321 | - | 9.2994 | 9.6921 | 9.9285 | 7.0167 | 7.5272 | 7.5399 |
| | $4^{th}$ | 17.0355 | - | 15.6762 | 16.0440 | 16.2860 | 12.1951 | 12.8912 | 12.8545 |
| | $5^{th}$ | 27.4868 | - | 23.5495 | 23.8728 | 24.1196 | 18.8430 | 19.6904 | 19.5969 |
| | $1^{st}$ | 1.0110 | 1.0110 | 1.5446 | 1.8278 | 1.9774 | 1.0474 | 1.2181 | 1.2702 |
| | $2^{nd}$ | 4.1740 | 4.1740 | 4.6445 | 5.0194 | 5.2322 | 3.3779 | 3.7440 | 3.7525 |
| 0.05 | $3^{th}$ | 9.8598 | 9.8598 | 9.7601 | 10.1345 | 10.3614 | 7.3780 | 7.9012 | 7.9060 |
| | $4^{th}$ | 18.6338 | - | 17.0446 | 17.3809 | 17.6073 | 13.2832 | 14.0186 | 13.9640 |
| | $5^{th}$ | 31.2018 | - | 26.5951 | 26.8736 | 27.1016 | 21.3127 | 22.2403 | 22.1147 |
| | $1^{st}$ | 1.0389 | 1.0389 | 1.5628 | 1.8431 | 1.9916 | 1.0623 | 1.2326 | 1.2838 |
| | $2^{nd}$ | 4.5952 | 4.5952 | 5.0033 | 5.3532 | 5.5536 | 3.6588 | 3.9955 | 4.0315 |
| 0.10 | $3^{th}$ | 11.8266 | 11.8266 | 11.4990 | 11.8171 | 12.0146 | 8.7368 | 9.3128 | 9.2904 |
| | $4^{th}$ | 24.3000 | - | 21.9395 | 22.1933 | 22.3809 | 17.1639 | 18.0516 | 17.9408 |
| | $5^{th}$ | 43.7693 | - | 36.9613 | 37.1361 | 37.3285 | 29.7045 | 30.9210 | 30.6978 |

**Table 4.** Dimensionless nonlocal frequencies of Clamped-Pinned (C-P) FG nanobeam for higher modes of vibrations.

| $\lambda_c$ / $\lambda_c$ | Mode | No Surface Effects | | Square Cross-Section | | | Circular Cross-Section | | |
|---|---|---|---|---|---|---|---|---|---|
| | | Present | Ref. [34] | $n=0$ | $n=1$ | $n=3$ | $n=0$ | $n=1$ | $n=3$ |
| | $1^{st}$ | 1.0000 | 1.0000 | 1.2776 | 1.4411 | 1.5296 | 0.8955 | 1.0101 | 1.0362 |
| | $2^{nd}$ | 3.2406 | 3.2406 | 3.4794 | 3.7020 | 3.8302 | 2.5552 | 2.7816 | 2.8020 |
| $0.00^{+}$ | $3^{th}$ | 6.7614 | 6.7614 | 6.6373 | 6.8740 | 7.0185 | 5.0325 | 5.3803 | 5.3797 |
| | $4^{th}$ | 11.5623 | - | 10.5625 | 10.7930 | 10.9466 | 8.2399 | 8.6987 | 8.6705 |
| | $5^{th}$ | 17.6435 | - | 15.0470 | 15.2594 | 15.4214 | 12.0630 | 12.5991 | 12.5415 |
| | $1^{st}$ | 1.0108 | - | 1.2883 | 1.4520 | 1.5407 | 0.9035 | 1.0186 | 1.0447 |
| | $2^{nd}$ | 3.2813 | - | 3.5167 | 3.7389 | 3.8670 | 2.5840 | 2.8118 | 2.8318 |
| 0.01 | $3^{th}$ | 6.8644 | - | 6.7266 | 6.9619 | 7.1059 | 5.1033 | 5.4539 | 5.4523 |
| | $4^{th}$ | 11.7807 | - | 10.7415 | 10.9692 | 11.1219 | 8.3852 | 8.8487 | 8.8187 |
| | $5^{th}$ | 18.0579 | - | 15.3677 | 15.5760 | 15.7366 | 12.3295 | 12.8723 | 12.8117 |
| | $1^{st}$ | 1.0375 | - | 1.3129 | 1.4763 | 1.5651 | 0.9221 | 1.0381 | 1.0639 |
| | $2^{nd}$ | 3.4104 | - | 3.6320 | 3.8504 | 3.9766 | 2.6734 | 2.9048 | 2.9230 |
| 0.03 | $3^{th}$ | 7.2715 | - | 7.0827 | 7.3084 | 7.4476 | 5.3834 | 5.7448 | 5.7382 |
| | $4^{th}$ | 12.7887 | - | 11.5928 | 11.8040 | 11.9489 | 9.0666 | 9.5542 | 9.5140 |

Preprints (www.preprints.org) | NOT PEER-REVIEWED | Posted: 10 January 2024 doi:10.20944/preprints202401.0738.v1



| | | | | | | | | | |
|---|---|---|---|---|---|---|---|---|---|
| | $5^{th}$ | 20.1774 | - | 17.0764 | 17.2602 | 17.4109 | 13.8938 | 14.3097 | 14.2316 |
| | $1^{st}$ | 1.0703 | 1.0703 | 1.3416 | 1.5041 | 1.5925 | 0.9442 | 1.0611 | 1.0864 |
| | $2^{nd}$ | 3.5967 | 3.5967 | 3.7972 | 4.0084 | 4.1311 | 2.8017 | 3.0378 | 3.0528 |
| 0.05 | $3^{th}$ | 7.9066 | 7.9066 | 7.6426 | 7.8527 | 7.9839 | 5.8222 | 6.2008 | 6.1861 |
| | $4^{th}$ | 14.4028 | - | 12.9725 | 13.1593 | 13.2927 | 10.1653 | 10.6941 | 10.6379 |
| | $5^{th}$ | 23.5687 | - | 19.8429 | 19.9935 | 20.1319 | 15.9729 | 16.6313 | 16.5260 |
| | $1^{st}$ | 1.1749 | 1.1749 | 1.4304 | 1.5875 | 1.6737 | 1.0131 | 1.1318 | 1.1418 |
| | $2^{nd}$ | 4.2468 | 4.2468 | 4.3784 | 4.5650 | 4.6750 | 3.2517 | 3.5049 | 3.5094 |
| 0.10 | $3^{th}$ | 10.1365 | 10.1365 | 9.6348 | 9.8008 | 9.9094 | 7.3762 | 7.8211 | 7.7804 |
| | $4^{th}$ | 19.9215 | - | 17.7410 | 17.8691 | 17.9770 | 13.9492 | 14.6302 | 14.5244 |
| | $5^{th}$ | 34.7602 | - | 29.0444 | 29.1236 | 29.2425 | 23.4328 | 24.3488 | 24.1620 |

**Table 5.** Dimensionless nonlocal frequencies of Doubly-Clamped (C-C) FG nanobeam for higher modes of vibrations.

| $\lambda_c$ | Mode | No Surface Effects | | Square Cross-Section | | | Circular Cross-Section | | |
|---|---|---|---|---|---|---|---|---|---|
| $\lambda_c$ | | Present | Ref. [34] | $n=0$ | $n=1$ | $n=3$ | $n=0$ | $n=1$ | $n=3$ |
| | $1^{st}$ | 1.0000 | 1.0000 | 1.1448 | 1.2397 | 1.2927 | 0.8225 | 0.9067 | 0.9181 |
| | $2^{nd}$ | 2.7565 | 2.7565 | 2.8670 | 3.0045 | 3.0849 | 2.1245 | 2.2952 | 2.3016 |
| $0.00^{+}$ | $3^{th}$ | 5.4039 | 5.4039 | 5.2236 | 5.3724 | 5.4652 | 3.9804 | 4.2402 | 4.2136 |
| | $4^{th}$ | 8.9329 | - | 8.0769 | 8.2231 | 8.3237 | 6.3237 | 6.6614 | 6.6334 |
| | $5^{th}$ | 13.3443 | - | 11.2860 | 11.4210 | 11.5289 | 9.0751 | 9.4637 | 9.4155 |
| | $1^{st}$ | 1.0214 | - | 1.1656 | 1.2606 | 1.3137 | 0.8382 | 0.9233 | 0.9345 |
| | $2^{nd}$ | 2.8211 | - | 2.9263 | 3.0633 | 3.1436 | 2.1703 | 2.3433 | 2.3491 |
| 0.01 | $3^{th}$ | 5.5464 | - | 5.3466 | 5.4941 | 5.5864 | 4.0783 | 4.3420 | 4.3320 |
| | $4^{th}$ | 9.2036 | - | 8.2957 | 8.4395 | 8.5393 | 6.5027 | 6.8459 | 6.8158 |
| | $5^{th}$ | 13.8141 | - | 11.6416 | 11.7729 | 11.8798 | 9.3734 | 9.7689 | 9.7176 |
| | $1^{st}$ | 1.0726 | - | 1.2135 | 1.3075 | 1.3603 | 0.8745 | 0.9615 | 0.9720 |
| | $2^{nd}$ | 3.0062 | - | 3.0942 | 3.2271 | 3.3054 | 2.3001 | 2.4789 | 2.4823 |
| 0.03 | $3^{th}$ | 6.0329 | - | 5.7732 | 5.9120 | 6.0001 | 4.4141 | 4.6914 | 4.6761 |
| | $4^{th}$ | 10.2718 | - | 9.1936 | 9.3233 | 9.4169 | 7.2234 | 7.5923 | 7.5524 |
| | $5^{th}$ | 15.8833 | - | 13.2967 | 13.4079 | 13.5077 | 10.5476 | 11.1652 | 11.0979 |
| | $1^{st}$ | 1.1349 | 1.1349 | 1.2701 | 1.3620 | 1.4138 | 0.9178 | 1.0066 | 1.0161 |
| | $2^{nd}$ | 3.2614 | 3.2614 | 3.3252 | 3.4508 | 3.5253 | 2.4786 | 2.6649 | 2.6648 |
| 0.05 | $3^{th}$ | 6.8814 | 6.8814 | 6.4143 | 6.5396 | 6.6208 | 4.9160 | 5.2143 | 5.1908 |
| | $4^{th}$ | 11.9129 | - | 10.5959 | 10.7059 | 10.7909 | 8.3411 | 8.7528 | 8.6978 |
| | $5^{th}$ | 19.0851 | - | 15.9012 | 15.9867 | 16.0780 | 12.8489 | 13.3540 | 13.2626 |
| | $1^{st}$ | 1.1766 | 1.1766 | 1.4485 | 1.5316 | 1.5790 | 1.0549 | 1.1487 | 1.1546 |
| | $2^{nd}$ | 4.1322 | 4.1322 | 4.1225 | 4.2251 | 4.2875 | 3.0922 | 3.3059 | 3.2939 |
| 0.10 | $3^{th}$ | 9.2325 | 9.2325 | 8.6431 | 8.7337 | 8.7977 | 6.6519 | 7.0286 | 6.9793 |
| | $4^{th}$ | 17.4074 | - | 15.3466 | 15.4132 | 15.4815 | 12.1120 | 12.6785 | 12.5778 |
| | $5^{th}$ | 29.4704 | - | 24.4213 | 24.4545 | 24.5363 | 19.7635 | 20.5082 | 20.3449 |

Preprints (www.preprints.org) | NOT PEER-REVIEWED | Posted: 10 January 2024 doi:10.20944/preprints202401.0738.v1



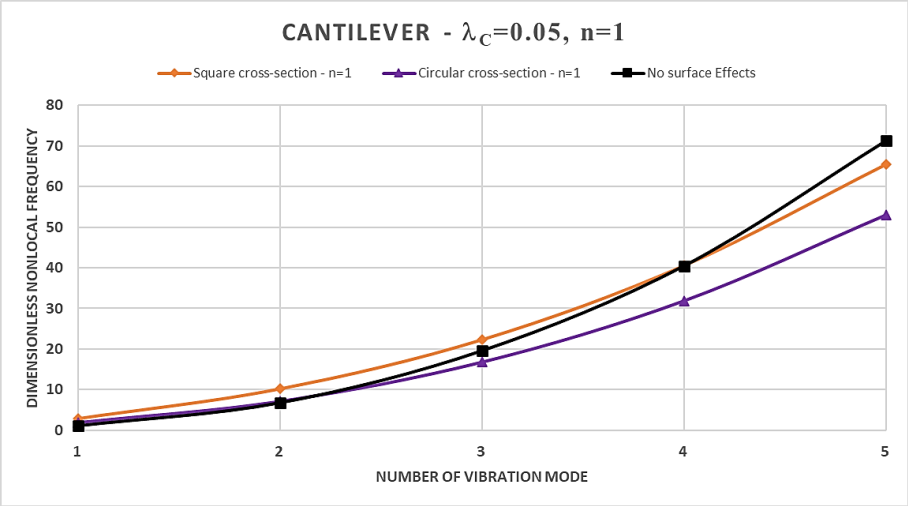


**Figure 2.** Dimensionless nonlocal frequencies of FG nanobeams vs. number of vibration modes evaluated for FG Cantilever (C-F) condition, with $\lambda_c = 0.05$ and $n = 1$.

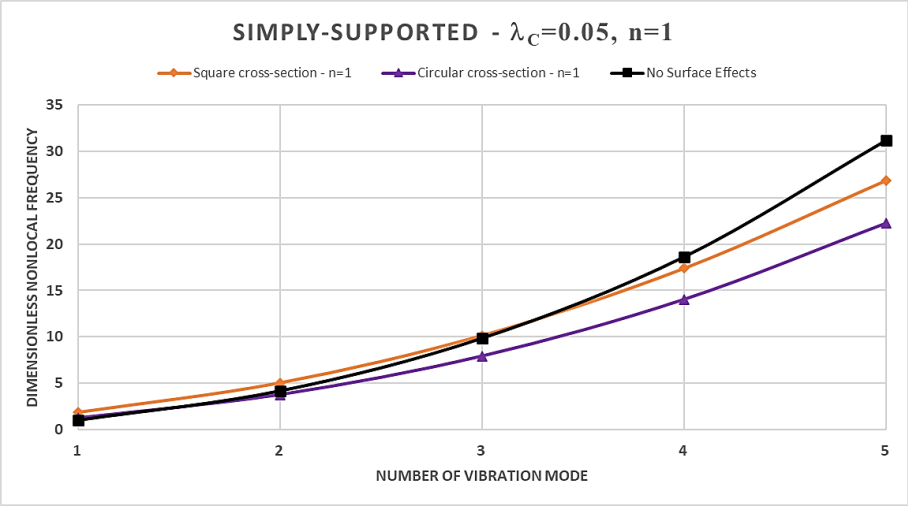


**Figure 3.** Dimensionless nonlocal frequencies of FG nanobeams vs. number of vibration modes evaluated for FG Simply-Supported (S-S) condition, with $\lambda_c = 0.05$ and $n = 1$.

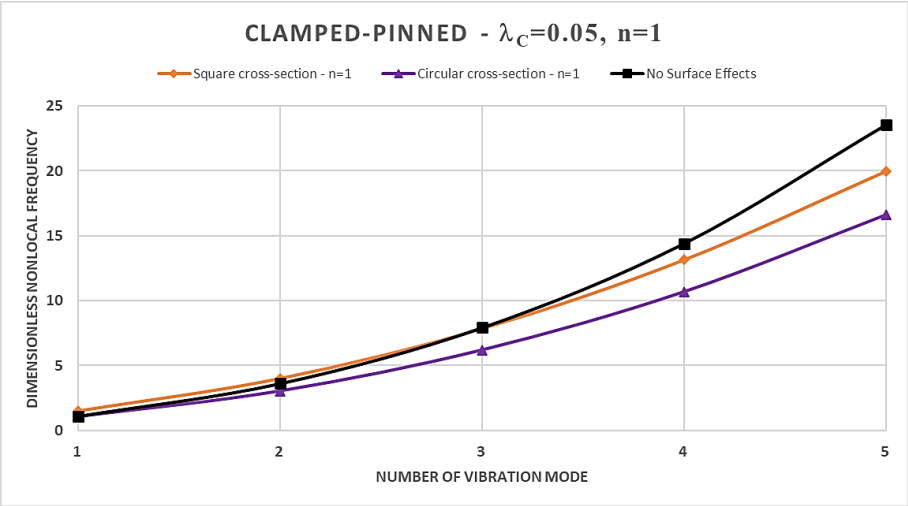


**Figure 4.** Dimensionless nonlocal frequencies of FG nanobeams vs. number of vibration modes evaluated for FG Clamped-Pinned (C-P) condition, with $\lambda_c = 0.05$ and $n = 1$.

Preprints (www.preprints.org) | NOT PEER-REVIEWED | Posted: 10 January 2024 doi:10.20944/preprints202401.0738.v1



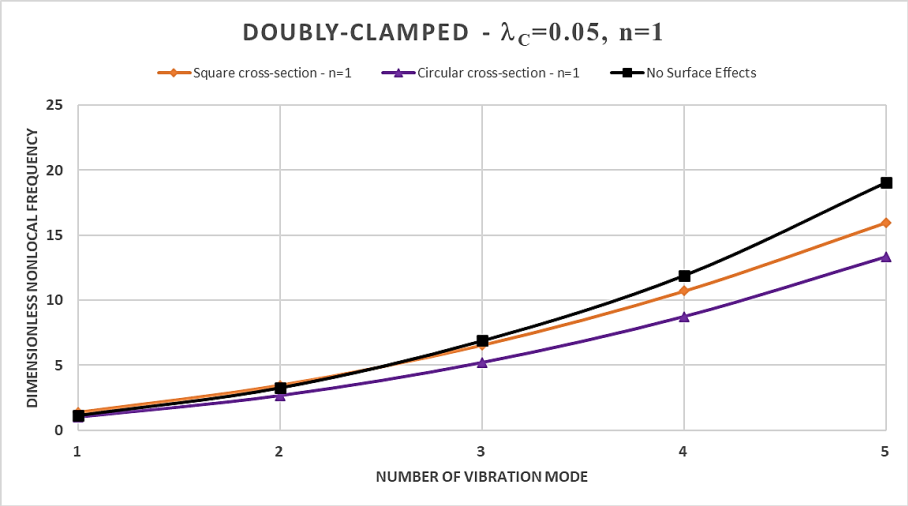


**Figure 5.** Dimensionless nonlocal frequencies of FG nanobeams vs. number of vibration modes evaluated for FG Doubly-Clamped (C-C) condition, with $\lambda_c = 0.05$ and $n = 1$.

## 5. Conclusions

This study presents the main results of an application of the surface-stress driven model developed to investigate the coupled influences of the nonlocal parameter and the material gradient index on the higher order free vibrations analysis of the functionally graded nanobeams. The analysis is conducted using a Wolfram language code developed in Mathematica by the authors.

The results have been successfully compared to those presented by Raimondo et al. in Ref. [34], where the surface energy effects have been neglected, confirming the accuracy and reliability of the proposed approach.

The main conclusions are the following:

- an increase in the material gradient index consistently results in an increase in the normalized nonlocal frequencies in the case of square cross-section, regardless of the boundary constrains are considered; while, for the case of the circular cross-section the trend is conditioned by the specific static scheme considered;
- the normalized nonlocal frequencies increase by increasing the order of the vibration modes for each static schemes considered;
- the dimensionless nonlocal frequencies reach their maximum value in the case of the C-F nanobeam and the minimum one in the case of C-C nanobeam for each vibration mode, regardless of the cross-sectional shapes chosen;
- the nonlocality strongly influences the dimensionless frequencies, and its effects are stronger for higher vibration modes;
- by increasing the nonlocal parameter, the SSDM formulation always shows an increase in the normalized nonlocal frequencies;
- as the number of vibration modes increases the SSDM model always provides a stiffening behavior;
- in the case of a square cross-section, the presence of surface effects results in additional stiffness, leading to an increase in the dimensionless normalized nonlocal frequencies for the first three vibration modes compared to the model without surface effects; however, the surface energy causes a reduction in dimensionless nonlocal frequencies for the fourth and fifth vibration modes;
- finally, the dynamic behavior of circular FG nanobeams is influenced by the coupled effects of the material gradient index and the nonlocal parameter, as well as by the boundary conditions at the nanobeams ends, and, therefore, it is not possible to define a specific trend.

approach in capturing surface energy effects within the full dynamic response of functionally graded Bernoulli-Euler nanobeams. This methodology provides a cost-effective means to design and optimize nanoscale structures, particularly applicable to nanoelectromechanical systems (NEMS).

**Author Contributions:** For research articles with several authors, a short paragraph specifying their individual contributions must be provided. The following statements should be used "Conceptualization, L.F. and R.P.; methodology, L.F., G.L. and R.P.; software, L.F., G.L. and R.P.; validation, L.F., G.L. and R.P.; formal analysis, L.F., A.L., G.L. and R.P.; Investigation, L.F., A.L., G.L. and R.P.; resources, L.F. and R.P.; data curation, L.F., A.L., G.L. and R.P.; writing—original draft preparation, L.F., A.L., G.L. and R.P.; writing—review and editing, L.F., A.L., G.L. and R.P.; visualization, A.L. and G.L.; supervision, L.F. and R.P.; project administration, L.F. and R.P.; funding acquisition, L.F. and R.P. All authors have read and agreed to the published version of the manuscript."

**Funding:** This research was funded by the Italian Ministry of University and Research (MUR), Research Grant PRIN 2020 No. 2020EBLPLS on "Opportunities and challenges of nanotechnology in advanced and green construction materials" and Research Grant PRIN 2022 "ISIDE: Intelligent Systems for Infrastructural Diagnosis in smart-concretE", N. 2022S88WAY - CUP B53D2301318.

**Data Availability Statement:** Not applicable.

**Acknowledgments:** The authors gratefully acknowledge the financial support of the Italian Ministry of University and Research (MUR), Research Grant PRIN 2020 No. 2020EBLPLS on "Opportunities and challenges of nanotechnology in advanced and green construction materials" and Research Grant PRIN 2022 "ISIDE: Intelligent Systems for Infrastructural Diagnosis in smart-concretE", N. 2022S88WAY - CUP B53D2301318.

**Conflicts of Interest:** "The authors declare no conflict of interest."

## References

1. Ö. Civalek, B. Uzun, M. Ö. Yaylı, "On nonlinear stability analysis of saturated embedded porous nanobeams", International Journal of Engineering Science, vol. 190, no. 103898, May 2023. DOI: https://doi.org/10.1016/j.ijengsci.2023.103898.
2. F. Cornacchia, F. Fabbrocino, N. Fantuzzi, R. Luciano, R. Penna, "Analytical solution of cross- and angle-ply nano plates with strain gradient theory for linear vibrations and buckling", Mech. Adv. Mater. Struct, vol. 28, no. 12, pp. 1201-1215, September 2019. DOI: 10.1080/15376494.2019.1655613.
3. X. Xu, D. Shahsavari, B. Karami, "On the forced mechanics of doubly-curved nanoshells", International Journal of Engineering Science,vol. 168, no. 103538, November 2021. DOI: https://doi.org/10.1016/j.ijengsci.2021.103538.
4. A. Gholipour, M. H. Ghayesh, "Nonlinear coupled mechanics of functionally graded nanobeams", International Journal of Engineering Science, vol. 150, no. 103221, May 2020. DOI: https://doi.org/10.1016/j.ijengsci.2020.103221.
5. B. Karami, M. Janghorban, "On the mechanics of functionally graded nanoshells", International Journal of Engineering Science, vol. 153, no. 103309, August 2020. DOI: https://doi.org/10.1016/j.ijengsci.2020.103309.
6. M. H. Ghayesh, A. Farajpour, "A review on the mechanics of functionally graded nanoscale and microscale structures", International Journal of Engineering Science, vol. 137, pp. 8-36, April 2019. DOI: https://doi.org/10.1016/j.ijengsci.2018.12.001.
7. A. Farajpour, M. H. Ghayesh, H. Farokhi, "A review on the mechanics of nanostructures", International Journal of Engineering Science, vol. 133, pp. 231-263, December 2018. DOI: https://doi.org/10.1016/j.ijengsci.2018.09.006.
8. H. Akhavan, M. Ghadiri, A. Zajkani, "A new model for the cantilever MEMS actuator in magnetorheological elastomer cored sandwich form considering the fringing field and casimir effects", Mechanical Systems and Signal Processing, vol. 121, pp. 551-561, April 2019. DOI: https://doi.org/10.1016/j.ymssp.2018.11.046.
9. D.C.C. Lam, F. Yang, A.C.M. Chong, J. Wang, P. Tong, "Experiments and theory in strain gradient elasticity", Journal of the Mechanics and Physics of Solids, vol. 51, no. 8, pp. 1477-1508, August 2003). DOI: https://doi.org/10.1016/S0022-5096(03)00053-X.
10. S. J. L. Billinge, I. Levin, "The Problem with Determining Atomic Structure at the Nanoscale", Science, vol. 316, no. 5824, pp. 561-565, April 2007. DOI: 10.1126/science.1135080.
11. A. Eringen, "Linear theory of nonlocal elasticity and dispersion of plane waves", Int J. Eng Sci, vol. 10, no. 5, pp. 425–435, May 1972.
12. A. Eringen, "On differential equations of nonlocal elasticity and solutions of screw dislocation and surface waves", J. Appl. Phys., vol. 54, pp. 4703-4710, September 1983.
13. Eringen A.C., 1987. Theory of nonlocal elasticity and some applications, Res Mechanica 21, 313-342.
14. C. Lim, G. Zhang, J.N. Reddy, "A higher-order nonlocal elasticity and strain gradient theory and its applications in wave propagation", J. Mech. Phys. Solids, vol. 78, pp. 298-313, May 2015. DOI:10.1016/j.jmps.2015.02.001.
15. R. Mindlin, "Micro-structure in linear elasticity", Archive for Rational Mechanics and Analysis, vol.16, no. 1, pp. 51–78, January 1964.

16. M. Gurtin, A. Murdoch, "A continuum theory of elastic material surfaces", Archive for Rational Mechanics and Analysis, vol. 57, no. 4, pp.291–323, December 1975.
17. M. Gurtin, A. Murdoch, "Surface stress in solids", International Journal of Solids and Structures, vol. 14, no. 6, pp. 431–440, November 1977. DOI: https://doi.org/10.1016/0020-7683(78)90008-2.
18. J. Fernández-Sáez, R. Zaera, J. Loya, J. Reddy, "Bending of Euler–Bernoulli beams using Eringen's integral formulation: A paradox resolved", International Journal of Engineering Science, vol. 99, pp. 107-116, February 2016. DOI: https://doi.org/10.1016/j.ijengsci.2015.10.013.
19. C. Li, L. Yao, W. Chen, S. Li, "Comments on nonlocal effects in nano-cantilever beams", International Journal of Engineering Science, vol. 87, pp. 47-57, February 2015. DOI: https://doi.org/10.1016/j.ijengsci.2014.11.006.
20. G. Romano, R. Barretta, R, "Comment on the paper ''Exact solution of Eringen's nonlocal integral model for bending of Euler–Bernoulli and Timoshenko beams by Meral Tuna & Mesut Kirca'', International Journal of Engineering Science, vol. 109, pp. 240–242, December 2016. DOI: https://doi.org/10.1016/j.ijengsci.2016.09.009.
21. G. Romano, R. Barretta, M. Diaco, F. Marotti de Sciarra, "Constitutive boundary conditions and paradoxes in nonlocal elastic nano-beams", International Journal of Mechanical Sciences, vol. 121, pp. 151–156, August 2017. DOI: 10.1016/j.ijmecsci.2016.10.036.
22. G. Romano and R. Barretta R., "Nonlocal elasticity in nanobeams: The stress-driven integral model", Int. J. Eng. Sci., vol. 115, pp. 14-27, June 2017. DOI:10.1016/j.ijengsci.2017.03.002.
23. R. Penna, L. Feo, G. Lovisi, "Hygro-thermal bending behavior of porous FG nano-beams via local/nonlocal strain and stress gradient theories of elasticity", Composite Structures, vol. 263, no. 113627, May 2021. DOI: 10.1016/j.compstruct.2021.113627.
24. R. Penna, L. Feo, G. Lovisi, F. Fabbrocino, "Hygro-Thermal Vibrations of Porous FG Nano-Beams Based on Local/Nonlocal Stress Gradient Theory of Elasticity", Nanomaterials, vol. 11, no. 910, March 2021. DOI:10.3390/nano11040910.
25. R. Penna, A. Lambiase, G. Lovisi and L. Feo, "Investigating hygrothermal bending behavior of FG nanobeams via local/nonlocal stress gradient theory of elasticity with general boundary conditions", Mech. Adv. Mater. Struct, October 2023. DOI: 10.1080/15376494.2023.2269938.
26. H. Darban, F. Fabbrocino, L. Feo, R. Luciano, "Size-dependent buckling analysis of nanobeams resting on two-parameter elastic foundation through stress-driven nonlocal elasticity model", Mech. Adv. Mater. Struct, vol. 28, March 2020. DOI:10.1080/15376494.2020.1739357.
27. A. Apuzzo, R. Barretta, R. Luciano, F. Marotti de Sciarra, R. Penna, "Free vibrations of Bernoulli-Euler nano-beams by the stress-driven nonlocal integral model", Composites Part B: Engineering, vol. 123, pp. 105-111, August 2017. DOI: https://doi.org/10.1016/j.compositesb.2017.03.057.
28. Caporale, H. Darban, and R. Luciano, Exact closed-form solutions for nonlocal beams with loading discontinuities, Mech. Adv. Mater. Struct., vol. 29, no. 5, pp. 694–704, 2022. DOI: 10. 1080/15376494.2020.1787565.
29. Y. Tang, and H. Qing, Bi-Helmholtz kernel based stress-driven nonlocal integral model with discontinuity for size-dependent fracture analysis of edge-cracked nanobeam, Mech. Adv. Mater. Struct., pp. 1–11, 2023. DOI: 10.1080/15376494.2023.2214922.
30. R. Barretta, L. Feo, L., R. Luciano, F. Marotti de Sciarra, R. Penna, "Nano-beams under torsion: a stress-driven nonlocal approach", PSU Research Review, vol. 1, no. 2, pp. 164-169, May 2017.DOI: https://doi.org/10.1108/PRR-05-2017-0030.
31. R. Penna, G. Lovisi, L. Feo, "Dynamic Response of Multilayered Polymer Functionally Graded Carbon Nanotube Reinforced Composite (FG-CNTRC) Nano-Beams in Hygro-Thermal Environment", Polymers, vol. 13, no. 2340, July 2021. DOI:10.3390/polym13142340.
32. Francesco Fabbrocino, Marco Francesco Funari, Fabrizio Greco, Paolo Lonetti, Raimondo Luciano, Rosa Penna, Dynamic crack growth based on moving mesh method,
Composites Part B: Engineering, Volume 174, 2019, 107053. DOI:10.1016/j.compositesb.2019.107053.
33. Andrea Apuzzo, Chiara Bartolomeo, Raimondo Luciano, Daniela Scorza, Novel local/nonlocal formulation of the stress-driven model through closed form solution for higher vibrations modes, Composite Structures, Volume 252, 2020, 112688. https://doi.org/10.1016/j.compstruct.2020.112688.
34. Raimondo Luciano, Hossein Darban, Chiara Bartolomeo, Francesco Fabbrocino, Daniela Scorza, Free flexural vibrations of nanobeams with non-classical boundary conditions using stress-driven nonlocal model, Mechanics Research Communications, Volume 107, 2020, 103536, https://doi.org/10.1016/j.mechrescom.2020.103536.
35. R. Penna, "Bending analysis of functionally graded nanobeams based on stress-driven nonlocal model incorporating surface energy effects", International Journal of Engineering Science, vol. 189, no. 103887, August 2023. DOI: 10.1016/j.ijengsci.2023.103887.

36. L. Feo, G. Lovisi and R. Penna, "Free vibration analysis of functionally graded nanobeams based on surface stress-driven nonlocal model", Mech. Adv. Mater. Struct, December 2023. https://doi.org/10.1080/15376494.2023.2289079.
37. Rosa Penna, Luciano Feo, Giuseppe Lovisi, Arturo Pascuzzo, A stress-driven model incorporating surface energy effects for the bending analysis of functionally graded nanobeams with loading discontinuities, Procedia Structural Integrity, Volume 47, 2023, Pages 789-799, ISSN 2452-3216, https://doi.org/10.1016/j.prostr.2023.07.040.
38. G. Lovisi, "Application of the surface stress-driven nonlocal theory of elasticity for the study of the bending response of FG cracked nanobeams", Composite Structures, vol. 324, no. 117549, November 2023. DOI: 10.1016/j.compstruct.2023.117549.
39. S. Saffari, M. Hashemian, D. Toghraie, "Dynamic stability of functionally graded nanobeam based on nonlocal Timoshenko theory considering surface effects", Physica B: Condensed Matter, vol. 520, pp. 97–105, September 2017. DOI: https://doi.org/10.1016/j.physb.2017.06.029.